



NIH PUBLIC ACCESS

Author Manuscript

Dev Biol. Author manuscript; available in PMC 2012 July 15.

Published in final edited form as:

Dev Biol. 2011 July 15; 355(2): 349–357. doi:10.1016/j.ydbio.2011.04.036.

Novel *cis*-regulatory function in ICR-mediated imprinted repression of *H19*

Folami Y. Ideraabdullah^{a,1}, Lara K. Abramowitz^{a,1}, Joanne L. Thorvaldsen^a, Christopher Krapp^a, Sherry C. Wen^{a,2}, Nora Engel^b, and Marisa S. Bartolomei^{a,*}

^aDepartment of Cell and Developmental Biology, University of Pennsylvania School of Medicine, 415 Curie Boulevard, Philadelphia, PA 19104 USA

^bFels Institute for Cancer Research and Molecular Biology, Temple University School of Medicine, 3307 North Broad Street, Philadelphia, PA 19140 USA

Abstract

Expression of coregulated imprinted genes, *H19* and *Igf2*, is monoallelic and parent-of-origin-dependent. Like most imprinted genes, *H19* and *Igf2* are regulated by a differentially methylated imprinting control region (ICR). CTCF binding sites and DNA methylation at the ICR have previously been identified as key *cis*-acting elements required for proper *H19/Igf2* imprinting. Here, we use mouse models to elucidate further the mechanism of ICR-mediated gene regulation. We specifically address the question of whether sequences outside of CTCF sites at the ICR are required for paternal *H19* repression. To this end, we generated two types of mutant ICRs in the mouse: (i) deletion of intervening sequence between CTCF sites (*H19^{ICRΔIVS}*), which changes size and CpG content at the ICR; and (ii) CpG depletion outside of CTCF sites (*H19^{ICR-8nrCG}*), which only changes CpG content at the ICR. Individually, both mutant alleles (*H19^{ICRΔIVS}* and *H19^{ICR-8nrCG}*) show loss of imprinted repression of paternal *H19*. Interestingly, this loss of repression does not coincide with a detectable change in methylation at the *H19* ICR or promoter. Thus, neither intact CTCF sites nor hypermethylation at the ICR is sufficient for maintaining the fully repressed state of the paternal *H19* allele. Our findings demonstrate, for the first time *in vivo*, that sequence outside of CTCF sites at the ICR is required in *cis* for ICR-mediated imprinted repression at the *H19/Igf2* locus. In addition, these results strongly implicate a novel role of ICR size and CpG density in paternal *H19* repression.

Keywords

Genomic imprinting; *H19*; DNA methylation; Transcriptional regulation; Imprinted repression; CpG density

© 2011 Elsevier Inc. All rights reserved.

*Corresponding author. Department of Cell and Developmental Biology, University of Pennsylvania School of Medicine, 415 Curie Boulevard, Philadelphia, PA 19104 USA. Telephone: (215) 898-9063, Fax: (215) 573-6434, bartolom@mail.med.upenn.edu.

¹These authors contributed equally to this work.

²Present address. Department of Microbiology, Vanderbilt School of Medicine, 215 Light Hall, Nashville, TN 37232 USA

Publisher's Disclaimer: This is a PDF file of an unedited manuscript that has been accepted for publication. As a service to our customers we are providing this early version of the manuscript. The manuscript will undergo copyediting, typesetting, and review of the resulting proof before it is published in its final citable form. Please note that during the production process errors may be discovered which could affect the content, and all legal disclaimers that apply to the journal pertain.

Introduction

Genomic imprinting is an epigenetic process resulting in monoallelic expression of a subset of mammalian genes. Expression of imprinted genes is dependent on the parent-of-origin of the allele (Cattanach and Kirk, 1985). During gametogenesis, parental alleles of imprinted genes are differentially marked with DNA methylation, which is maintained throughout development despite genome-wide demethylation in the preimplantation embryo (Oswald et al., 2000; Tremblay et al., 1997). Loss of imprinting is often associated with loss of differential methylation and is implicated in many human diseases, including several types of cancers (Gicquel et al., 2005; Sparago et al., 2007; Wu et al., 2006).

Most imprinted genes reside in clusters throughout the genome (Verona et al., 2003), which allows for coregulation of closely located genes. One of the first identified and most widely studied clusters is located on distal mouse chromosome 7 and found in conserved synteny on human chromosome 11. Located in this region are imprinted genes *H19* (a non-coding RNA of unknown function) and *Igf2* (a fetal mitogen), which are expressed from alternate parental alleles but share elements controlling their imprinted expression (Bartolomei et al., 1991; DeChiara et al., 1991; Thorvaldsen et al., 1998). Loss of imprinting at this locus is associated with Beckwith-Wiedemann Syndrome (BWS), an over-growth syndrome linked to overexpression or biallelic expression of *IGF2* (Cerrato et al., 2008; Sparago et al., 2007); and the reciprocal disorder, Silver-Russell Syndrome (SRS), a dwarfism syndrome linked to underexpression or biallelic silencing of *IGF2* (Gicquel et al., 2005).

Imprinted expression of *H19* and *Igf2* in the mouse is regulated by two key elements: (i) shared enhancers downstream of *H19* including those that control expression in endodermal (Leighton et al., 1995) and mesodermal (Kaffer et al., 2001; Kaffer et al., 2000) tissues and (ii) a differentially methylated imprinting control region (ICR) located between the two genes, -2 to -4 kb from the *H19* transcriptional start site (Thorvaldsen et al., 1998; Tremblay et al., 1997).

Differential methylation at the ICR is established during germ cell development when parental alleles are separated. At this time maternal and paternal alleles become hypo- and hyper-methylated, respectively (Davis et al., 2000; Tremblay et al., 1997). CTCF binds the hypomethylated maternal ICR at four tandem repetitive sites (Bell and Felsenfeld, 2000b; Hark et al., 2000a), establishing an insulator that blocks *Igf2* promoters from interaction with the downstream enhancers. This binding prevents maternal *Igf2* expression and allows maternal *H19* expression (Engel et al., 2006; Pant et al., 2003; Szabo et al., 2004). Conversely, CTCF does not bind to the hypermethylated paternal ICR, allowing interaction between *Igf2* and downstream enhancers and subsequent expression of paternal *Igf2* (Bell and Felsenfeld, 2000a; Hark et al., 2000b).

Previous studies have demonstrated roles for both *cis* and *trans*-acting elements at the ICR in regulation of *H19* expression. On the maternal allele, studies clearly show that binding of CTCF to the ICR is required for insulation and activation of maternal *H19* (Engel et al., 2006; Schoenherr et al., 2003; Szabo et al., 2004). Less is known about the regulatory function of the hypermethylated paternal ICR in *H19* repression. DNA methylation at the ICR plays a major role in paternal *H19* repression and it has been proposed that the hypermethylated ICR acts as a center for spreading repressive methylation to the *H19* promoter thereby silencing paternal *H19* (Thorvaldsen et al., 1998; Tremblay et al., 1997). Based on *in vitro* assays, Chen et al. reported that the positions of CpGs within CTCF binding sites at the ICR are more important for repression than positions of CpGs outside of CTCF binding sites (Chen et al., 2009). Furthermore, we showed that paternal inheritance of a CpG depleted ICR (mutation of 9 CpGs within CTCF binding sites, *H19*^{DMD-9CG})

resulted in hypomethylation at the mutant ICR and biallelic *H19* expression (Engel et al., 2004).

In addition to DNA methylation, *in vitro* assays as well as mutations at the endogenous locus provide evidence that the ICR may harbor other elements that repress *H19* expression (Chen et al., 2009; Drewell et al., 2000; Engel et al., 2004). In particular, a 1.2 kb region was reported to be a silencer element (Brenton et al., 1999; Lyko et al., 1997). Deletion of this region on the paternal allele resulted in a loss of *H19* repression without a change in methylation at the ICR in E13.5 embryos (Drewell et al., 2000). This deletion removed two CTCF binding sites and ~50% of the ICR, containing more than 50% of methylation sites (CpGs). Therefore, it is not known whether size, CpG content or CTCF binding sites are responsible for this silencer function.

These and other studies clearly demonstrate that *cis*-acting elements at the ICR are required for paternal repression. However, because all reported *in vivo* mutations that disrupt *H19* paternal repression also disrupted CTCF binding sites, it remains unclear whether repression is solely dependent upon sequence at CTCF binding sites, or if sequences outside of CTCF binding sites are also important in *H19* repression. Here, we specifically investigated the presence of *cis*-acting repressive elements within the *H19* ICR but outside of CTCF binding sites. We analyzed the effects of two mutations at the ICR on paternal *H19* repression: (1) deletion of sequence between CTCF binding sites 2 and 3 (*H19*^{ICR-ΔIVS}), which reduces the size of the ICR and depletes CpGs and potential binding sites for *trans*-acting factors without disrupting CTCF binding sites, and (2) CpG depletion at the ICR but outside of CTCF sites, with no change in size of the ICR (*H19*^{ICR-8nrCG}). Paternal inheritance of both *H19*^{ICR-8nrCG} and *H19*^{ICR-ΔIVS} leads to loss of repression of paternal *H19* indicating that the ICR acts in *cis* through size and CpG density, independent of CTCF binding sites, to repress paternal *H19* expression.

Materials and Methods

Targeting vectors

pH19^{ICRΔIVS}neo (Figure 1A): Using a 2.2 kb 129/SvJ genomic fragment containing the *H19* ICR [from *HindIII*, -2.06 kb upstream of the *H19* transcription start site (TSS) to *HindIII*, -4.3 kb upstream of the *H19* TSS] cloned into pBluescriptIIKSM (pBSIIKSM), 0.873 kb of intervening sequence (IVS) between CTCF sites 2 and 3 (from *BglII* site at -2.7 kb and *BspHI* site at -3.6 kb) was deleted by Quikchange site-directed mutagenesis (Stratagene). Primer used for site directed mutagenesis: 5'-GTGAGCCACACTGGCTGGGATATCATAGATGGTGATAGGGGAG - 3' (AT nucleotides added at site of deletion generate an *EcoRV* site for Southern blot analysis to confirm targeting). Deletion of IVS was confirmed by sequencing with primers that flank the deleted sequence: Primer1F, 5'-GCAACTTCGGTCTTACCAGCCACT-3' and Primer1R, 5'-TGCAAGGAGACCATGCCCTATTCTTG -3'. The fragment containing the IVS deletion was excised from the endogenous *KpnI* site, -3.7 kb upstream of *H19* TSS to the *KpnI* site in pBSIIKSM and inserted at a unique *KpnI* site of the previously described targeting vector [TVΔDMDneo (Thorvaldsen et al., 1998), modified to remove *KpnI* site in pBSIIKSM]. As described previously (Thorvaldsen et al., 1998), the targeting vector also contained a neomycin resistance (*neo*^r) gene cassette (for selection) flanked by *loxP* sites and pBSIIKSM. Informative restriction enzyme digestions followed by agarose gel electrophoresis were used to confirm accurate insertion and orientation of the mutated fragment within the targeting vector.

pH19^{ICR-8nrCG}neo (Figure 1A): A129/SvJ genomic DNA fragment spanning the *H19* ICR [described previously (Engel et al., 2004)] was mutated at each of the four regions indicated

below using the Quikchange site-directed mutagenesis kit (Stratagene) :
 GTACCTCGTGGACT[CG->CA]GACTC, TGGTGATTTG[CG->GC]CTTT[CG->GC]TAT, ACACAGCC[CG->CT]AGAT[CG->CT]TCAGT, CCTTCA[CG->CT]AT[CG->CT]AT[CG->CT]GTTCA (mutations italicized). The targeting vector was generated as described previously (Engel et al., 2004) using this mutated ICR in place of the DMD-9CG mutation. Informative restriction enzyme digestions followed by agarose gel electrophoresis were used to confirm accurate insertion and orientation of the mutated fragment within the targeting vector and mutated CpGs were confirmed by sequencing.

Embryonic Stem (ES) cells and mouse generation

Targeting vectors were linearized and electroporated into E14.1 ES cells (Kuhn 1991) as described previously (Thorvaldsen et al., 1998). G418-resistant positive clones were isolated and targeting to the *H19/Igf2* locus was confirmed by restriction digestion followed by Southern hybridization as described previously (Thorvaldsen et al., 1998). Correctly targeted ES cell clones were injected into C57BL/6J (B6) blastocysts and mice were generated by the Transgenic & Chimeric Mouse Facility at the University of Pennsylvania. Chimeras were obtained and mated to B6 mice. Germline transmission of the targeted mutant alleles was confirmed in the agouti progeny by DNA isolated from tail biopsies subjected to Southern blot as described previously (Thorvaldsen et al., 1998). All studies adhered to procedures approved by the Institutional Animal Care and Use Committee at the University of Pennsylvania.

Mouse breeding and genotyping

Mutant mice having inherited the targeted mutations through germline transmission were confirmed by PCR based genotyping on DNA isolated from tail biopsies using primers that flank the deletion (Primer1F and Primer1R, as described above, for the Δ IVS mutation) or using primers that flank the end of the *Neo^r* cassette (Primer2F, 5' - CGAAGTTATTAGGTCCCTCGATCGAG - 3' and Primer2R, 5' - CACCCCATGACCCTTATGAATCATTG - 3' for both the Δ IVS and 8nrCG alleles). The *neo^r* cassette (flanked by loxP sites) was excised in the mouse by crossing heterozygous mutant mice (*H19^{ICR} Δ IVS^{Neo/+}* or *H19^{ICR}8nrCG^{Neo/+}*) to mice expressing Cre recombinase under the control of the human cytomegalovirus promoter on a B6 genetic background (obtained from Edward Morissey). *Neo^r* excision was confirmed in the progeny by Southern blot and PCR analysis using primers that flank the *neo^r* cassette, G2 (H19-2.3F) and G5 (H19-2.0F), as described previously (Thorvaldsen et al., 1998; Thorvaldsen et al., 2002). Mutant lines lacking the *neo^r* cassette were maintained by crossing to B6 and selecting for progeny carrying the mutation by PCR analysis. To distinguish parental alleles for all allelic assays described in this study, heterozygous mutant mice (*H19^{ICR} Δ IVS^{+/+}* or *H19^{ICR}8nrCG^{+/+}*) were crossed to B6(CAST7), also referred to as C7 mice, which are homozygous on chromosome 7 for wild-type alleles from the *Mus musculus castaneus* (CAST) strain on a mostly B6 background (Mann et al., 2003). Mice were weighed immediately after birth to determine the presence of abnormal growth as has been associated with loss of imprinting at *Igf2*. Unless otherwise indicated, for all experiments, mutant mice are compared to their wild-type littermate controls.

DNA isolation and methylation analysis

DNA was isolated from neonatal liver and mature sperm as described previously (Bartolomei 1993). Methylation Southern analysis was performed as described previously (Thorvaldsen et al., 2002). Bisulfite mutagenesis was performed on liver and sperm according to the manufacturer's protocol of the MOD50 Imprint® DNA Modification Kit (SIGMA-ALDRICH). For wild-type and 8nrCG bisulfite converted samples, R1 & R2 were amplified as described previously (Davis et al., 2000) using primers BMsp2t1, BMsp2t2,

BHhalt4 and BHhalt3 with the following modification to BHhalt4 (5' - CTAACCTCATAAAACCCATAACTAT - 3'); and R3 was amplified using BHha5t2, BHha5t, and BHha5t3. For Δ IVS samples R1, R2 and R3 were amplified using primers BMsp2t1 and Primer3R1 (BUP4R) 5' - AATAAATCAAATTCTCTAATTCAATATA - 3' followed by nested primer with, BMsp2t2 and BHha5t3 (Davis et al., 2000). For wild-type, 8nrCG and Δ IVS samples, R4 was amplified as described previously (Thorvaldsen et al., 2002) using B8 (BTV3-1), B9 (BTV3-2), B10 (BTV3-3) and B11 (BTV3-4); and the *H19* promoter proximal region was amplified as described previously (Thorvaldsen et al., 2006) using B12 (BH19-0.9f), B13 (BH19-0.85f) and B14 (BH19-0.5r).

RNA isolation and analysis

Total RNA was extracted from mouse tissues of various developmental stages (tissues used fresh or flash frozen in liquid nitrogen and stored at -80°C) using Trizol Reagent (Invitrogen) and by following the manufacturer's protocol. For *H19* RNase protection assay (RPA), 5 μg of RNA was used with the RPAIII RNase protection assay kit (Ambion) following manufacturer's protocol. The probe was prepared and analysis performed as described previously (Thorvaldsen et al., 1998).

For reverse transcription PCR (RT-PCR), RNA was first DNase treated using RQ1 DNase (Promega) according to manufacturer's protocol, and next reverse transcribed using Superscript III (Invitrogen) following manufacturer's protocol. For each RNA sample, both negative (no transcriptase added) and positive (transcriptase added) were performed. Approximately 2.5ng of cDNA was used for all assays. For allele specific RT-PCR, *Igf2* was amplified using primers Igf2-18 and Igf2-20 and digested with restriction enzyme *Tsp4091*, as previously described (Thorvaldsen et al., 2006). *H19* was amplified using primers HE2 and HE4 (Thorvaldsen et al., 2006), which amplifies a 235 bp fragment. Alleles were specified using a nucleotide polymorphism between the B6 and CAST alleles that generates a *Cac8I* site unique to B6. When digested with *Cac8I*, the CAST allele is 235 bp while the B6 fragments were 173 bp and 62 bp. Digested RT-PCR fragments were resolved on either 15% (*Igf2*) or 12% (*H19*) polyacrylamide gel and band intensities were measured using ImageJ. For quantitative (q) RT-PCR, total *Igf2* levels were measured in reference to *Arpp0* (*acidic phosphoprotein P0 subunit*) as previously described (Weaver et al., 2010).

Statistics

P-value calculated using two-tailed Student's T-test with equal variance to compare the percent paternal *H19* expression between *H19*^{ICR Δ IVS} and *H19*^{ICR-8nrCG} alleles shown in Figure 2.

Results

Generation of the *H19*^{ICR Δ IVS} and *H19*^{ICR-8nrCG} alleles

To determine the presence of *cis*-regulatory elements outside of CTCF sites at the *H19* ICR, mice carrying two types of mutant alleles at the endogenous locus were generated by homologous recombination in ES cells: *H19*^{ICR Δ IVS} and *H19*^{ICR-8nrCG}. The sequence perturbed by these mutations is not conserved between rodents and humans (Frevel et al., 1999; Stadnick et al., 1999), however, the *H19*^{ICR Δ IVS} deletion removes ~ 0.9 kb of sequence between CTCF sites 2 and 3 at the ICR, which reduces the size of the ICR by $\sim 50\%$ and deletes $\sim 35\%$ of the CpGs at the ICR (Figure 1A); and the *H19*^{ICR-8nrCG} allele contains mutations in 8 CpGs across the ICR, which depletes $\sim 16\%$ of CpGs without changing the size of the ICR or disrupting CTCF sites (Figure 1A). Two of the eight CpGs mutated in the 8nrCG mutant overlap with the Δ IVS deletion.

Germline transmission of the targeted clones and excision of the *neo^r* cassette in the mouse was confirmed by Southern blot analysis (Figure 1B). Mutant progeny lacking the *neo^r* cassette were assayed for defects in *H19/Igf2* imprinting when the mutant allele was maternally or paternally inherited. In the experiments described below, parental origin of alleles was distinguished by crossing heterozygous mutant mice (*H19^{ICRΔIVS/+}* or *H19^{ICR-8nrCG/+}*) to wild-type C7 mice. Tissues from the resulting heterozygous mutant neonatal progeny were compared to their heterozygous wild-type littermates.

Paternal inheritance of *H19^{ICRΔIVS}* and *H19^{ICR-8nrCG}* mutations results in derepression of paternal *H19*

To determine the effects of the Δ IVS and 8nrCG mutations on imprinting at the *H19/Igf2* locus we assayed allelic expression by RNase Protection Assay (RPA). Upon paternal inheritance of either *H19^{ICRΔIVS}* or *H19^{ICR-8nrCG}*, paternal *H19* expression, indicative of loss of imprinting, was observed in neonatal liver (Figure 2A) and at very low levels in tongue (Figure 2B). Paternal *H19* levels were consistently higher [though not always significantly higher (p=.07 in liver, p=.01 in tongue)] in the 8nrCG mutants compared to Δ IVS (Figure 2A and 2B). This aberrant paternal *H19* expression was detectable as early as E13.5 in embryonic tissues when either mutant was paternally transmitted (Figure 3 and data not shown); and in extraembryonic tissues as early as E6.5 and E13.5 in 8nrCG and Δ IVS mutants, respectively (Figure 3 and data not shown). Despite biallelic expression of *H19*, no size difference was observed when comparing wild-type and mutant (*H19^{ICRΔIVS}* or *H19^{ICR-8nrCG}*) neonates within litters (data not shown). Furthermore, both qRT-PCR and northern blot analysis revealed no difference in total *Igf2* expression levels in liver of mutant and wild-type littermates (Figure 2C and data not shown).

Aberrant paternal *H19* expression observed in *H19^{ICRΔIVS}* and *H19^{ICR-8nrCG}* mutants is subject to the temporally and spatially restricted expression pattern of *H19*

Derepression of the paternal allele in *H19^{ICRΔIVS}* and *H19^{ICR-8nrCG}* mutants is not detectable at all developmental time points and tissues when *H19* is normally expressed. Therefore, we next examined whether the expression pattern of the mutant *H19/Igf2* locus follows the temporally restricted pattern of the wild-type locus or if a *de novo* mechanism is activating the mutant locus. To this end, we first determined whether the level of expression of paternal *H19* observed in association with the mutant ICRs is correlated with the total level of *H19* expression observed at different developmental time points.

In the mouse, *H19* expression levels vary between developmental stages. *H19* is detectable as early as E3.5 in trophoctoderm and E8.5 in the embryo proper (Doherty et al., 2000; Poirier et al., 1991). Levels steadily increase thereafter to peak around 3 days after birth and remain high until day 9 before rapidly declining to basal levels by day 28 (Pachnis et al., 1984). By analyzing levels of paternal *H19* expression in liver throughout development, we found that for both mutations the stage of development when total *H19* is expressed at its highest level, neonatal liver (Pachnis et al., 1984), is also when aberrant paternal *H19* expression is highest (Figure 3). Likewise, when total *H19* is at intermediate (E13.5) or very low levels (4 wks) (Pachnis et al., 1984), aberrant paternal *H19* expression in the mutant is also at intermediate or undetectable levels (Figure 3). These data demonstrate that aberrant paternal *H19* expression levels positively correlate with the temporally restricted expression pattern of *H19*.

In addition to examining the effects of our mutations at different developmental stages, we also analyzed *H19* expression in embryonic vs. extraembryonic mutant tissues at a single developmental time (E13.5) in comparison to wild-type littermates (Figure 3). We observed paternal *H19* derepression in all three tissues tested (E13.5 liver, placenta and yolk sac).

Interestingly, the levels of aberrant paternal *H19* expression appear more variable among extraembryonic samples (E13.5 yolk sac and placenta) than observed among the embryonic samples (E13.5 liver) (Figure 3). Overall, this finding confirms that the aberrant paternal *H19* expression pattern associated with the Δ IVS and 8nrCG mutation coincides with the spatially restricted expression pattern of *H19*.

Taken together, we conclude that the level of paternal *H19* derepression associated with the *H19*^{ICR- Δ IVS} and *H19*^{ICR-8nrCG} mutant alleles is dependent upon the levels of total *H19* expression and is not regulated by a *de novo* temporal or tissue specific mechanism. Thus, the effects of these mutations are specifically due to a disruption in imprinted repression of *H19*.

Derepression of paternal H19 occurs in the absence of changes to establishment or maintenance of epigenetic modifications at the ICR or H19 promoter

Biallelic *H19* expression is often indicative of a loss of methylation at the paternal ICR and/or *H19* promoter (Engel et al., 2004; Thorvaldsen et al., 1998). To determine whether paternal *H19* methylation was perturbed by the Δ IVS or 8nrCG mutations, we performed bisulfite sequencing at the ICR in neonatal liver. We observed no significant changes in DNA methylation at the mutant paternal ICRs as compared to the wild-type ICRs in littermates (Figure 4A), demonstrating that neither mutation disrupts maintenance of the hypermethylated paternal ICR. Next, we determined whether these mutations affect methylation establishment at the ICR in mature sperm. We have previously determined that methylation around CTCF sites 1 & 2 is representative of the entire ICR, therefore we only investigated these regions. There was no observable defect in hypermethylation at the paternal ICR in mutant sperm compared to wild-type sperm (Figure 4A).

Bisulfite analysis clearly demonstrates that the Δ IVS and 8nrCG mutations do not affect hypermethylation at the ICR. However, to determine the effects of these mutations on spreading of methylation to the *H19* promoter, we analyzed methylation at the *H19* promoter (by Southern blot analysis) and promoter proximal regions (by bisulfite sequencing) in neonatal liver. Interestingly, though we did see activation of paternal *H19* in these mutant tissues, we were unable to detect loss of methylation as compared to wild-type littermates either at the *H19* promoter proximal region or at the *H19* promoter (Figure 4A & B, respectively). These data demonstrate that although both *H19*^{ICR- Δ IVS} and *H19*^{ICR-8nrCG} mutant alleles are able to properly establish and maintain the hypermethylated status of the paternal *H19/Igf2* locus, imprinted *H19* repression is perturbed.

Analysis of maternal transmission of *H19*^{ICR Δ IVS} and *H19*^{ICR-8nrCG} alleles

We next assessed the effects of maternal inheritance of either the *H19*^{ICR Δ IVS} or *H19*^{ICR-8nrCG} alleles using allele specific RT-PCR. We observed that both mutants properly express *Igf2* monoallelically from the paternal allele (Figure 2D). Additionally, using bisulfite mutagenesis and sequencing we found that both *H19*^{ICR Δ IVS} and *H19*^{ICR-8nrCG} mutant maternal alleles were properly hypomethylated at the ICR (data not shown). No difference in weight was observed when comparing wild-type and mutant neonatal littermates for either mutant (data not shown). We thus conclude that maternal inheritance of either mutant allele does not disrupt imprinting at the *H19/Igf2* locus.

Discussion

Genomic imprinting is a complex epigenetic phenomenon that is an essential part of normal development. It requires that cellular machinery first recognize the parental origin of nearly identical alleles and then differentially regulate allelic expression based on the parental

origin. More than 100 genes have been characterized as imprinted. Interestingly, despite this common outcome in gene expression, several mechanisms of imprinting have been described (Ideraabdullah et al., 2008). These include insulators and non-coding RNA mechanisms acting at the level of single loci, entire domains or even at entire chromosomal regions (ie. imprinted X inactivation).

At most imprinted loci it is well understood that ICRs play a key role in regulation of imprinted expression of linked genes. While research has provided many major breakthroughs in our understanding of ICR-mediated imprinting control, it is still not fully understood how ICRs regulate imprinting. This is true especially for genes like *H19* & *Igf2*, which are mainly regulated by the same ICR and enhancers but are expressed from opposite parental alleles. For this purpose, the *H19/Igf2* ICR plays dual roles: (1) insulation and *H19* activation on the maternal allele and (2) *Igf2* repression on the paternal allele.

Here we used two targeted mutations in the mouse, *H19^{ICRΔIVS}* and *H19^{ICR-8nrCG}*, to investigate the role of sequences at the ICR that are outside of CTCF binding sites. While these mutations had no observable effect on the maternal allele in insulation and activation, the mutations allowed us to specifically dissect the role of size and CpG content at the *H19* ICR in paternal *H19* repression. Derepression of paternal *H19* has been shown to occur by either loss of methylation at the paternal ICR and *H19* promoter or by formation of an insulator at an aberrantly demethylated paternal ICR (Engel et al., 2004; Thorvaldsen et al., 1998; Thorvaldsen et al., 2002). Surprisingly, we have found that while we can detect aberrant paternal *H19* expression in the *H19^{ICRΔIVS}* and *H19^{ICR-8nrCG}* mutants, methylation at the paternal ICR and *H19* promoter is unaffected. This finding demonstrates that while methylation at the paternal *H19* promoter and ICR is required for *H19* repression, it is clearly not sufficient. Therefore, the ICR contains a repressive function aside from its hypermethylated state and CTCF binding sites. Furthermore, this novel repressive function is particularly required when *H19* is expressed at very high levels (Figure 3).

The precise mechanism of this repressive function of the ICR remains unclear; however, our findings strongly support a role for ICR size and CpG content in repression of paternal *H19*. As shown in Figure 5, the 8nrCG mutations deplete ~16% of CpGs at the ICR without changing the ICR size while the Δ IVS mutation decreases the ICR size by ~50% thereby decreasing the overall number of CpGs by ~35% but actually increasing the CpG density by ~30%. Interestingly, while both mutants show derepression of paternal *H19*, we consistently observed slightly higher levels of aberrant paternal *H19* expression in *H19^{ICR-8nrCG}* vs. *H19^{ICRΔIVS}* mutant neonatal liver (Figure 2 A and B, and Figure 3). We propose that the reduced size of the Δ IVS mutant ICR causes it to be insufficient for maintaining complete repression of paternal *H19*, however, the higher CpG density at the Δ IVS mutant ICR permits better maintenance of the ICR's repressive function compared to the 8nrCG mutant ICR, which has lowered CpG density. Thus, the size and percent of CpGs at the 8nrCG and Δ IVS mutant ICRs are directly correlated with their ability to maintain paternal *H19* repression.

These findings elucidate a novel role of ICR-mediated repression on the paternal allele that has long been under speculation. It is not, however, conclusive whether ICR size and CpG content are the only repressive *cis*-acting elements at the ICR required for paternal *H19* repression. For example, the involvement of CTCF sites at the ICR in paternal *H19* repression also remains in question. Though numerous mutations have been made and characterized at the endogenous *H19* ICR, the role of ICR size and CpG content could not be determined as all previous mutations that reduce CpG content or ICR size simultaneously perturbed CTCF binding sites. Previously, Drewell and colleagues reported the presence of a 1.2 kb silencer element at the distal end of the *H19* ICR that is required for paternal *H19*

repression (Drewell et al., 2000). However, the repressive function of this silencer element at the endogenous mouse locus remains uncertain due to the fact that initial studies characterizing this element were performed in *Drosophila* (Lyko et al., 1997) and later studies determined that a *Drosophila* specific factor, Su (Hw), regulates the silencer activity (Schoenfelder and Paro, 2004). Interestingly, analogous to our mutants, targeted deletion of this silencer element (*H19^{SilK}*) at the paternal *H19* ICR also significantly reduces the number and density of CpGs (Figure 5) and resulted in derepression of paternal *H19* without a change in DNA hypermethylation at the remaining ICR sequence (Drewell et al., 2000). It is important to note that the Δ IVS mutation overlaps this silencer element by only ~300bp (~25% of the silencer element size, Figure 5). The 8nrCG mutations overlap the silencer element mutation at 5 bp and overlap the Δ IVS mutation at 4 bp (Figure 5). Additionally, no sequence mutations are common to the three mutants (Figure 5). Thus, although the mutated regions differ greatly among the three mutants (*H19^{SilK}*, *H19^{ICRAIVS}* and *H19^{ICR-8nrCG}*), paternal *H19* repression is significantly disrupted in all three, arguing against the presence of a single specific repressive element at the ICR.

These data strongly imply that it is not a particular region of the ICR (binding/other site) that harbors repressive elements but rather the overall size of the ICR and CpG density that play a significant role in repression of paternal *H19*. Though it can be argued that the 8nrCG and Δ IVS mutations may have disrupted binding of repressors or created a binding site for an activator, we do not believe this to be the case. Binding sites for sequence-specific repressors at the ICR are not likely to mediate repression for two reasons. First, other than CTCF sites, sequence at the ICR is poorly conserved among species (Frevel et al., 1999; Stadnick et al., 1999) and second, several attempts (through chromatin immunoprecipitation, DNA footprinting, etc.) to identify repressive factors that bind to the paternal *H19* ICR have returned few and unclear results (Reese et al., 2007; Szabo et al., 2000). Moreover, while it is also possible that these mutations have created binding sites for activators, this too is also unlikely due to the fact that several different types of mutations (deletions and point mutations) made in different regions of the ICR with very little sequence overlap have produced a similar loss of paternal *H19* repression.

The size and CpG content at the *H19* ICR varies widely among species. For example, the human *H19* ICR (imprinting center 1, IC1) is twice as large as the mouse (~5 kb vs. ~ 2 kb, respectively) and contains more than three times as many CpGs. It would be interesting to determine whether the differences in ICR size and CpG density between species is correlated to differences in the level of imprinted repressive function of the ICR. It will also be important to determine whether there is a specific effective size and CpG density that are sufficient for paternal *H19* repression and whether these two factors are equally important. In other words, is there a certain threshold for ICR size or CpG density that is sufficient to maintain repression or is it additive such that the level of repression is positively correlated with the ICR size and CpG density? Although further experiments are required, our data suggest the latter, an additive mechanism that is dependent on the size of the ICR and the density of CpGs therein.

Our studies further clarify the previously elusive repressive function of the *H19/Igf2* ICR, however, the specific factors responsible remain unknown. Of relevance, methyl-binding domain proteins, MeCP2 and MBD3, have been implicated in imprinting regulation at *H19/Igf2* (Drewell et al., 2002; Reese et al., 2007). It is likely that in addition to inhibiting binding of the activator/insulator CTCF, the repressive function of methylation at the *H19/Igf2* ICR also includes recruitment of repressive methyl-binding proteins. Therefore, even though changes in the paternal ICR size or subtle changes to CpG density (such as those caused by the 8nrCG mutation) may not be sufficient to cause significant defects in hypermethylation at the paternal ICR, they may be sufficient to disrupt/alter binding of

repressive factors such as methyl-binding proteins. Furthermore, a decrease in recruitment or binding of methyl-binding domain proteins may allow for a loosening of local chromatin which could potentially explain the derepression of paternal *H19* observed in this study. Further studies to examine just how CpG density, size of methylated ICRs, repressive protein complexes and local chromatin structure work together to cause repression at imprinted loci may have a wider implication in the repressive role of CpG clusters genome-wide.

In addition to exploring the mechanism of the repressive function of the *H19* ICR, these studies highlight the importance of studying the effects of subtle genetic perturbations in disease etiology. While most studies of SRS have identified epimutations at the IC1 as the major cause of defects in paternal *H19* repression associated with the disease (Bartholdi et al., 2009; Begemann et al., 2010; Gicquel et al., 2005); the 8nrCG mutant presented here suggests that single base pair mutations may also play a key role in aberrant transcriptional regulation at the *H19/Igf2* imprinted locus. It is, however, likely that in the case of such subtle genetic changes, secondary genetic/epigenetic mutations or human exposure to environmental factors may be required to cause the increased phenotypic effects associated with the disease state. This may also be relevant for larger genetic mutations. Interestingly, the Δ IVS mutation described here, which deletes previously identified Oct-binding sequences (Hori et al., 2002) that are conserved in humans and recently found to be mutated in BWS patients (Demars et al., 2010), does not affect imprinting at the locus when maternally inherited. This finding suggests that either the Oct-binding sequences are unimportant for ICR function on the maternal allele in the mouse and possibly in humans, or that additional perturbation of the genome (environmental or other) is required for loss of imprinting at the *H19/Igf2* locus. Further studies that combine mutant models or include environmental perturbation may be necessary to generate more analogous mouse models of human diseases such as SRS and BWS.

Acknowledgments

We thank Edward E. Morrisey for providing the Cre mice and Jean Richa and the University of Pennsylvania Transgenic Core Facility for the production of chimeric mice. This work was supported by NIH postdoctoral training grant (T32HD007516) and Ruth L. Kirschstein National Research Service Award (F32GM085999) to FYI, T32GM008216 (LKA) and GM51279 (MSB).

References

- Bartholdi D, Krajewska-Walasek M, Ounap K, Gaspar H, Chrzanowska KH, Ilyana H, Kayserili H, Lurie IW, Schinzel A, Baumer A. Epigenetic mutations of the imprinted IGF2-H19 domain in Silver-Russell syndrome (SRS): results from a large cohort of patients with SRS and SRS-like phenotypes. *J Med Genet.* 2009; 46:192–197. [PubMed: 19066168]
- Bartolomei MS, Zemel S, Tilghman SM. Parental imprinting of the mouse *H19* gene. *Nature.* 1991; 351:153–155. [PubMed: 1709450]
- Begemann M, Spengler S, Kanber D, Haake A, Baudis M, Leisten I, Binder G, Markus S, Rupprecht T, Segerer H, Fricke-Otto S, Muhlenberg R, Siebert R, Buiting K, Eggermann T. Silver-Russell patients showing a broad range of ICR1 and ICR2 hypomethylation in different tissues. *Clin Genet.* 2010
- Bell AC, Felsenfeld G. Methylation of a CTCF-dependent boundary controls imprinted expression of the *Igf2* gene. *Nature.* 2000a; 405:482–485. [PubMed: 10839546]
- Bell AC, Felsenfeld G. Methylation of a CTCF-dependent boundary controls imprinted expression of the *Igf2* gene. *Nature.* 2000b; 405:482–485. [PubMed: 10839546]
- Brenton JD, Drewell RA, Viville S, Hilton KJ, Barton SC, Ainscough JF, Surani MA. A silencer element identified in *Drosophila* is required for imprinting of H19 reporter transgenes in mice. *Proc Natl Acad Sci U S A.* 1999; 96:9242–9247. [PubMed: 10430927]

- Cattanach BM, Kirk M. Differential activity of maternally and paternally derived chromosome regions in mice. *Nature*. 1985; 315:496–498. [PubMed: 4000278]
- Cerrato F, Sparago A, Verde G, De Crescenzo A, Citro V, Cubellis MV, Rinaldi MM, Boccutto L, Neri G, Magnani C, D'Angelo P, Collini P, Perotti D, Sebastio G, Maher ER, Riccio A. Different mechanisms cause imprinting defects at the IGF2/H19 locus in Beckwith-Wiedemann syndrome and Wilms' tumour. *Hum Mol Genet*. 2008; 17:1427–1435. [PubMed: 18245780]
- Chen Y, Dhupelia A, Schoenherr CJ. The Igf2/H19 imprinting control region exhibits sequence-specific and cell-type-dependent DNA methylation-mediated repression. *Nucleic Acids Res*. 2009; 37:793–803. [PubMed: 19074953]
- Davis TL, Yang GJ, McCarrey JR, Bartolomei MS. The *H19* methylation imprint is erased and reestablished differentially on the parental alleles during male germ cell development. *Hum. Mol. Genet*. 2000; 9:2885–2894. [PubMed: 11092765]
- DeChiara TM, Robertson EJ, Efstratiadis A. Parental imprinting of the mouse insulin-like growth factor II gene. *Cell*. 1991; 64:849–859. [PubMed: 1997210]
- Demars J, Shmela ME, Rossignol S, Okabe J, Netchine I, Azzi S, Cabrol S, Le Caignec C, David A, Le Bouc Y, El-Osta A, Gicquel C. Analysis of the IGF2/H19 imprinting control region uncovers new genetic defects, including mutations of OCT-binding sequences, in patients with 11p15 fetal growth disorders. *Hum Mol Genet*. 2010; 19:803–814. [PubMed: 20007505]
- Doherty AS, Mann MRW, Tremblay KD, Bartolomei MS, Schultz RM. Differential effects of culture on imprinted *H19* expression in the preimplantation mouse embryo. *Biol Reprod*. 2000; 62:1526–1535. [PubMed: 10819752]
- Drewell RA, Brenton JD, Ainscough JF, Barton SC, Hilton KJ, Arney KL, Dandolo L, Surani MA. Deletion of a silencer element disrupts *H19* imprinting independently of a DNA methylation epigenetic switch. *Development*. 2000; 127:3419–3428. [PubMed: 10903168]
- Drewell RA, Goddard CJ, Thomas JO, Surani MA. Methylation-dependent silencing at the *H19* imprinting control region by MeCP2. *Nucleic Acids Res*. 2002; 30:1139–1144. [PubMed: 11861904]
- Engel N, Thorvaldsen JL, Bartolomei MS. CTCF binding sites promote transcription initiation and prevent DNA methylation on the maternal allele at the imprinted *H19/Igf2* locus. *Hum Mol Genet*. 2006; 15:2945–2954. [PubMed: 16928784]
- Engel NI, West AE, Felsenfeld G, Bartolomei MS. Antagonism between DNA hypermethylation and enhancer-blocking activity at the *H19 DMD* is revealed by CpG mutations. *Nature Genet*. 2004; 36:883–888. [PubMed: 15273688]
- Frevel MAE, Hornberg JJ, Reeve AE. A potential imprint control element: identification of a conserved 42 bp sequence upstream of *H19*. *Trends Genet*. 1999; 15:216–218. [PubMed: 10354581]
- Gicquel C, Rossignol S, Cabrol S, Houang M, Steunou V, Barbu V, Danton F, Thibaud N, Le Merrer M, Burglen L, Bertrand AM, Netchine I, Le Bouc Y. Epimutation of the telomeric imprinting center region on chromosome 11p15 in Silver-Russell syndrome. *Nat Genet*. 2005; 37:1003–1007. [PubMed: 16086014]
- Hark AT, Schoenherr CJ, Katz DJ, Ingram RS, Levorse JM, Tilghman SM. CTCF mediates methylation-sensitive enhancer-blocking activity at the *H19/Igf2* locus. *Nature*. 2000a; 405:486–489. [PubMed: 10839547]
- Hark AT, Schoenherr CJ, Katz DJ, Ingram RS, Levorse JM, Tilghman SM. CTCF mediates methylation-sensitive enhancer-blocking activity at the *H19/Igf2* locus. *Nature*. 2000b; 405:486–489. [PubMed: 10839547]
- Hori N, Nakano H, Takeuchi T, Kato H, Hamaguchi S, Oshimura M, Sato K. A dyad oct-binding sequence functions as a maintenance sequence for the unmethylated state within the *H19/Igf2*-imprinted control region. *J Biol Chem*. 2002; 277:27960–27967. [PubMed: 12029086]
- Ideraabdullah FY, Vigneau S, Bartolomei MS. Genomic imprinting mechanisms in mammals. *Mutat Res*. 2008; 647:77–85. [PubMed: 18778719]
- Kaffer CR, Grinberg A, Pfeifer K. Regulatory mechanisms at the mouse *Igf2/H19* locus. *Mol Cell Biol*. 2001; 21:8189–8196. [PubMed: 11689707]

- Kaffer CR, Srivastava M, Park K-Y, Ives E, Hsieh S, Batle J, Grinberg A, Huang S-P, Pfeifer K. A transcriptional insulator at the imprinted *H19/Igf2* locus. *Genes Dev.* 2000; 14:1908–1919. [PubMed: 10921905]
- Leighton PA, Saam JR, Ingram RS, Stewart CL, Tilghman SM. An enhancer deletion affects both *H19* and *Igf2* expression. *Genes Dev.* 1995; 9:2079–2089. [PubMed: 7544754]
- Lyko F, Brenton JD, Surani MA, Paro R. An imprinting element from the mouse H19 locus functions as a silencer in *Drosophila*. *Nat Genet.* 1997; 16:171–173. [PubMed: 9171828]
- Mann MRW, Chung YG, Nolen LD, Verona RI, Latham KE, Bartolomei MS. Disruption of imprinted gene methylation and expression in cloned preimplantation stage mouse embryos. *Biol Reprod.* 2003; 69:902–914. [PubMed: 12748125]
- Oswald J, Engemann S, Lane N, Mayer W, Olek A, Fundele R, Dean W, Reik W, Walter J. Active demethylation of the paternal genome in the mouse zygote. *Curr Biol.* 2000; 10:475–478. [PubMed: 10801417]
- Pachnis V, Belayew A, Tilghman SM. Locus unlinked to α -fetoprotein under the control of the murine *raf* and *Rif* genes. *Proc. Natl. Acad. Sci. USA.* 1984; 81:5523–5527. [PubMed: 6206499]
- Pant V, Mariano P, Kanduri C, Mattsson A, Lobanenko V, Heuchel R, Ohlsson R. The nucleotides responsible for the direct physical contact between the chromatin insulator protein CTCF and the H19 imprinting control region manifest parent of origin-specific long-distance insulation and methylation-free domains. *Genes Dev.* 2003; 17:586–590. [PubMed: 12629040]
- Poirier F, Chan C-TJ, Timmons PM, Robertson EJ, Evans MJ, Rigby PWJ. The murine H19 gene is activated during embryonic stem cell differentiation in vitro and at the time of implantation in the developing embryo. *Development.* 1991; 113:1105–1114. [PubMed: 1811930]
- Reese KJ, Lin S, Verona RI, Schultz RM, Bartolomei MS. Maintenance of paternal methylation and repression of the imprinted H19 gene requires MBD3. *PLoS Genetics.* 2007; 3:e137. [PubMed: 17708683]
- Schoenfelder S, Paro R. *Drosophila* Su(Hw) regulates an evolutionarily conserved silencer from the mouse H19 imprinting control region. *Cold Spring Harb Symp Quant Biol.* 2004; 69:47–54. [PubMed: 16117632]
- Schoenherr CJ, Levorske JM, Tilghman SM. CTCF maintains differential methylation at the *Igf2/H19* locus. *Nat Genet.* 2003; 33:66–69. [PubMed: 12461525]
- Sparago A, Russo S, Cerrato F, Ferraiuolo S, Castorina P, Selicorni A, Schwienbacher C, Negrini M, Ferrero GB, Silengo MC, Anichini C, Larizza L, Riccio A. Mechanisms causing imprinting defects in familial Beckwith-Wiedemann syndrome with Wilms' tumour. *Hum Mol Genet.* 2007; 16:254–264. [PubMed: 17158821]
- Stadnick MP, Pieracci FM, Cranston MJ, Taksel E, Thorvaldsen JL, Bartolomei MS. Role of a 461 bp G-rich repetitive element in *H19* transgene imprinting. *Dev. Genes Evo.* 1999; 209:239–248.
- Szabo P, Tang SH, Rentsendorj A, Pfeifer GP, Mann JR. Maternal-specific footprints at putative CTCF sites in the H19 imprinting control region give evidence for insulator function. *Curr Biol.* 2000; 10:607–610. [PubMed: 10837224]
- Szabo PE, Tang SH, Silva FJ, Tsark WM, Mann JR. Role of CTCF binding sites in the *Igf2/H19* imprinting control region. *Mol Cell Biol.* 2004; 24:4791–4800. [PubMed: 15143173]
- Thorvaldsen JL, Duran KL, Bartolomei MS. Deletion of the *H19* differentially methylated domain results in loss of imprinted expression of *H19* and *Igf2*. *Genes Dev.* 1998; 12:3693–3702. [PubMed: 9851976]
- Thorvaldsen JL, Fedoriw AM, Nguyen S, Bartolomei MS. Developmental profile of H19 differentially methylated domain (DMD) deletion alleles reveals multiple roles of the DMD in regulating allelic expression and DNA methylation at the imprinted H19/Igf2 locus. *Mol Cell Biol.* 2006; 26:1245–1258. [PubMed: 16449639]
- Thorvaldsen JL, Mann MR, Nwoko O, Duran KL, Bartolomei MS. Analysis of sequence upstream of the endogenous H19 gene reveals elements both essential and dispensable for imprinting. *Mol Cell Biol.* 2002; 22:2450–2462. [PubMed: 11909940]
- Tremblay KD, Duran KL, Bartolomei MS. A 5' 2-kilobase-pair region of the imprinted mouse *H19* gene exhibits exclusive paternal methylation throughout development. *Mol. Cell. Biol.* 1997; 17:4322–4329. [PubMed: 9234689]

- Verona RI, Mann MR, Bartolomei MS. Genomic imprinting: intricacies of epigenetic regulation in clusters. *Annu Rev Cell Dev Biol.* 2003; 19:237–259. [PubMed: 14570570]
- Weaver JR, Sarkisian G, Krapp C, Mager J, Mann MR, Bartolomei MS. Domain-specific response of imprinted genes to reduced DNMT1. *Mol Cell Biol.* 2010; 30:3916–3928. [PubMed: 20547750]
- Wu D, Li T, Lu Z, Dai W, Xu M, Lu L. Effect of CTCF-binding motif on regulation of PAX6 transcription. *Invest Ophthalmol Vis Sci.* 2006; 47:2422–2429. [PubMed: 16723452]

Research Highlights

- Sequence outside of CTCF sites at the ICR is required for imprinted *H19* repression.
- Hypermethylation of the paternal *H19* ICR is insufficient for full *H19* repression.
- *H19* ICR size and CpG density play a major role in paternal *H19* repression.

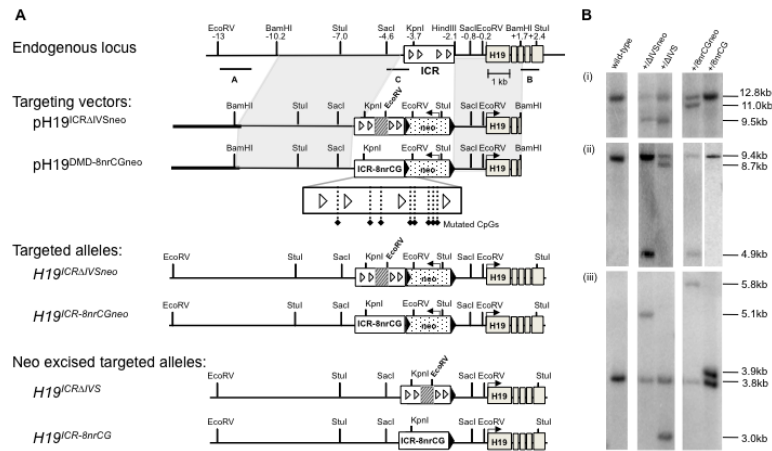
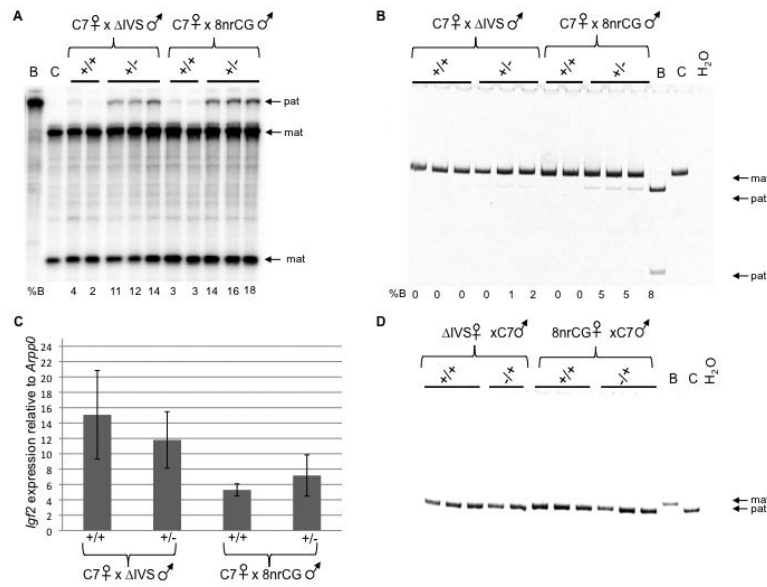


Figure 1. Generation of the at *H19^{ICR-8nrCG}* and *H19^{ICRΔIVS}* alleles. (A) Targeting scheme at the *H19/Igf2* locus. Illustrated from top to bottom are the wild-type locus, the targeting vectors, the correctly targeted alleles and the targeted alleles after excision of the *neo^r* selection marker. Restriction sites and their relative positions (in kb) to the *H19* transcription start site are indicated above the endogenous locus. Southern probes (A, B and C) are indicated by horizontal lines below the endogenous locus. Depicted is the endogenous sequence with the *H19* ICR (white rectangle), CTCF sites (white triangles) and *H19* exons (grey rectangles). The vectors include pBluescriptIIKS sequence (bold line), *neo^r* cassette (polka dot box), *loxP* sites (black arrowheads) and 129/Sv *H19* DNA (thin line). The deleted sequence in the ICR Δ IVS mutation is indicated by a cross-hatched region and the inserted *EcoRV* site (see materials and methods) is above locus in bold and diagonal. The CpG mutations in the ICR-8nrCG mutation are indicated by black diamonds. (B) Southern blots to confirm correctly targeted alleles using external probes A - *EcoRV* digest (i) and B - *StuI* digest (ii), and internal probe C - *SacI* digest (iii) as previously described (Thorvaldsen et al., 2002).

**Figure 2.**

Expression of *H19* and *Igf2* in ΔIVS or 8nrCG mutant neonatal tissues. (A) Allelic *H19* expression analyzed by RNase Protection Assay on neonatal liver RNA from heterozygous littermates having a maternally inherited CAST allele and either a paternally inherited mutant (+/-) or wild-type (+/+) B6 allele. (B) Allelic *H19* expression analyzed by RT-PCR and restriction enzyme digestion using neonatal tongue cDNA from heterozygous littermates as described above. The progeny tested were generated through crosses between C7 females and heterozygous mutant males ($H19^{ICR\Delta IVS/+}$ or $H19^{ICR-8nrCG/+}$) as indicated above panels. B6 (B) and CAST (C) controls are indicated. Arrows denote bands representative of paternal (pat) and maternal (mat) *H19* expression. The percent of *H19* expression from the mutant allele in each sample is indicated below each row (%B). (C) Total *Igf2* expression assayed by qRT-PCR on neonatal liver cDNA from heterozygous mutant and wild-type littermates as described above. *Igf2* mean relative expression levels (n=3) are displayed and standard deviation error bars are shown. (D) Allele specific *Igf2* expression was analyzed by RT-PCR using neonatal liver cDNA from heterozygous littermates carrying a paternally inherited CAST allele and either a maternally inherited mutant (-/+) or wild-type (+/+) B6 allele. The progeny tested were generated through crosses between heterozygous mutant females ($H19^{ICR\Delta IVS/+}$ or $H19^{ICR-8nrCG/+}$) and C7 males as indicated above panels. Negative RT controls showed no contamination for all RT-PCRs (data not shown).

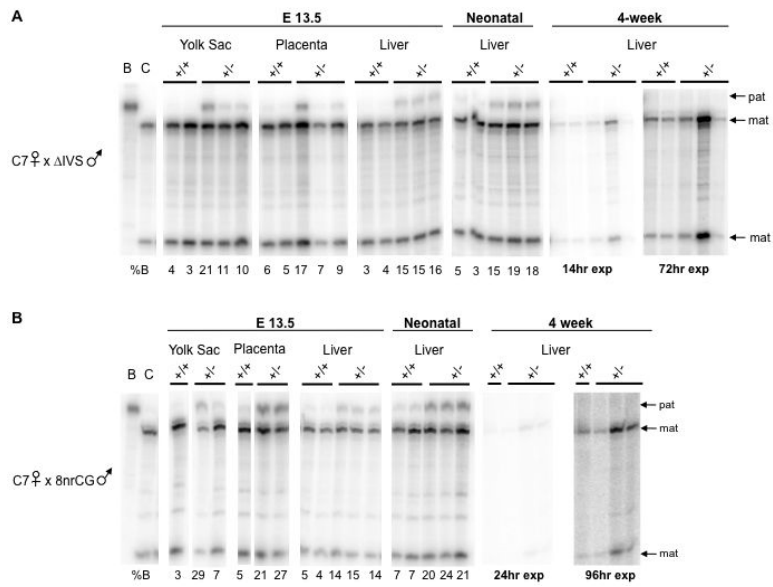


Figure 3. Paternal *H19* expression throughout development in Δ IVS or 8nrCG mutants. Allelic *H19* expression was analyzed by RNase Protection Assay in tissues harvested at different developmental times or tissues (as indicated). RNA was assayed from heterozygous littermates carrying a maternally inherited (mat) CAST (C) allele and either a paternally inherited (pat) mutant B6 (B) allele (+/-) or a paternally inherited wild-type B6 allele (+/+). The progeny tested were generated through crosses between C7 females and heterozygous mutant males [*H19*^{ICR Δ IVS/+} (A) or *H19*^{ICR-8nrCG/+} (B)] as indicated beside panels. Assay for 4-week liver is shown at normal exposure [14-24 hours (hrs), same as neonatal and embryonic tissues] to demonstrate low levels of expression at this time point, and overexposure (72-96hrs) to determine paternal allele expression. See legend to Figure 2 for details on percent allelic expression.

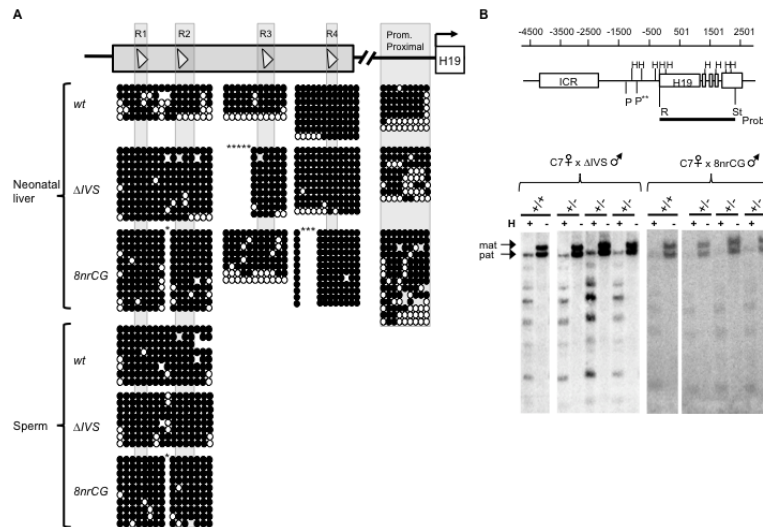


Figure 4. Methylation profile of the paternal *H19* and 5' upstream region in neonatal liver and sperm. (A) Schematic of the *H19* ICR and promoter proximal region (above, not drawn to scale). CTCF sites (triangles, R1–R4) at the ICR (horizontal grey rectangle) and promoter proximal region are depicted. Illustrated below is the methylation status of the mutant paternal *H19*^{ICRΔIVS} (Δ IVS) or *H19*^{ICR-8nrCG} (8nrCG) alleles and wild-type (*wt*) paternal alleles as determined by bisulfite mutagenesis and sequencing performed with neonatal liver and mature sperm. Open and closed circles denote unmethylated and methylated cytosines, respectively, along a single horizontal strand of cloned DNA. Absent circles indicate missing/undetermined sequence and asterisks (*) denote sequence deleted or mutated in the respective mutant alleles. Shaded rectangles overlay cytosines assayed in regions (CTCF sites or promoter proximal) indicated in above schematic. (B) Schematic of the *H19* region analyzed by methylation sensitive Southern blot [modified from (Thorvaldsen et al., 2002)]. The position (in base pairs) relative to the start of transcription is depicted above. Illustrated are: the endogenous *H19* transcription unit and ICR (rectangles); *Hpa*II (H) restriction sites; the polymorphic *Pvu*II (P) site denoted by asterisks (**); and the probe used (bold line below *H19* transcription unit) - *Eco*RI (R) to *Stu*I (St). Illustrated below, parental alleles were differentiated by digesting genomic DNA from neonatal liver with *Pvu*II, *Stu*I and *Hpa*II (+) or with only *Pvu*II and *Stu*I (-). Genotypes of the sample and the presence (+) or absence (-) of *Hpa*II (H) is marked above the panels. The progeny tested are littermates generated through crosses between C7 females and heterozygous mutant males (*H19*^{ICRΔIVS/+} or *H19*^{ICR-8nrCG/+}) as indicated above panels. The maternal (mat) CAST allele is 3.4 kb and the paternal (pat) B6 allele is 3.2 kb.

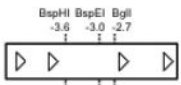
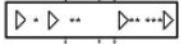

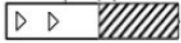
Allele	ICR size (bp)	CpG content			ICR
		#	%	%Δ	
Wild-type (B6)	1746	51	5.84%	--	
8nrCG	1746	43	4.93%	-15.58%	
ΔIVS	873	33	7.56%	+29.45%	
SILK@	901	22	4.88%	-16.44%	

Figure 5.

Comparison of ICR size and CpG content of *H19*^{ICR-8nrCG}, *H19*^{ICRΔIVS}, *H19*^{SILK} alleles. Symbol @ denotes reference for *H19*^{SILK} allele (Drewell et al., 2000). ICR size is shown as determined by number of base pairs (bp) from the start of the 21 bp consensus CTCF site 1, -3.9 kb upstream of *H19*, to the end of the 21 bp consensus CTCF site 4, -2.2 kb upstream of *H19* (149,766,207 - 149,767,952, NCBI m37). CpG content is categorized by number of CG dinucleotides within the ICR described above (#); the percent of CpGs (%) calculated by dividing the number (#) of CG dinucleotides by the total number of dinucleotides; and the percent change in CpG density between the mutant and wild-type ICRs (% Δ) calculated by subtracting the wild-type percent of CpGs (%) from the mutant percent of CpGs and dividing the final value by the wild-type percent of CpGs. The ICR is depicted for each allele: restriction sites and their relative positions (in kb) to the *H19* transcription start site are indicated above the endogenous locus, CTCF sites are denoted by triangles, deleted sequence in the adjacently described mutant ICR is indicated by cross-hatched regions and CpG mutations are indicated by asterisks.